Electronic Supplementary Material (ESI) for Journal of Materials Chemistry C.

Conformationally rigid molecular and polymeric naphthalene-diimides containing $C_6H_6N_2$ constitutional isomers†

Vincenzo Mirco Abbinante,[a] Gonzalo García-Espejo,[a] Gabriele Calabrese,[b] Silvia Milita,[b,*] Luisa Barba[c], Diego Marini[b], Candida Pipitone,[d] Francesco Giannici, [d] Antonietta Guagliardi[e,*] and Norberto Masciocchi[a,*]

Supporting Information

Supplementary Charts: Chart S1

Supplementary Figures: Figures S1-S23

Supplementary Tables: Tables S1-S6

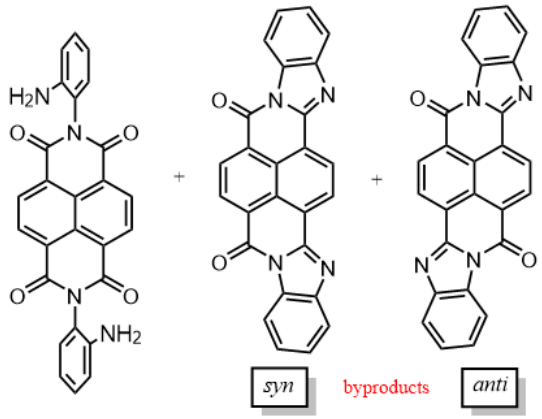

Chart S1. Sketch of the targeted NopDI molecule and of the condensation byproducts Pigment Red 194 and Pigment Orange molecules (the *syn*- and *anti*-isomers, respectively).

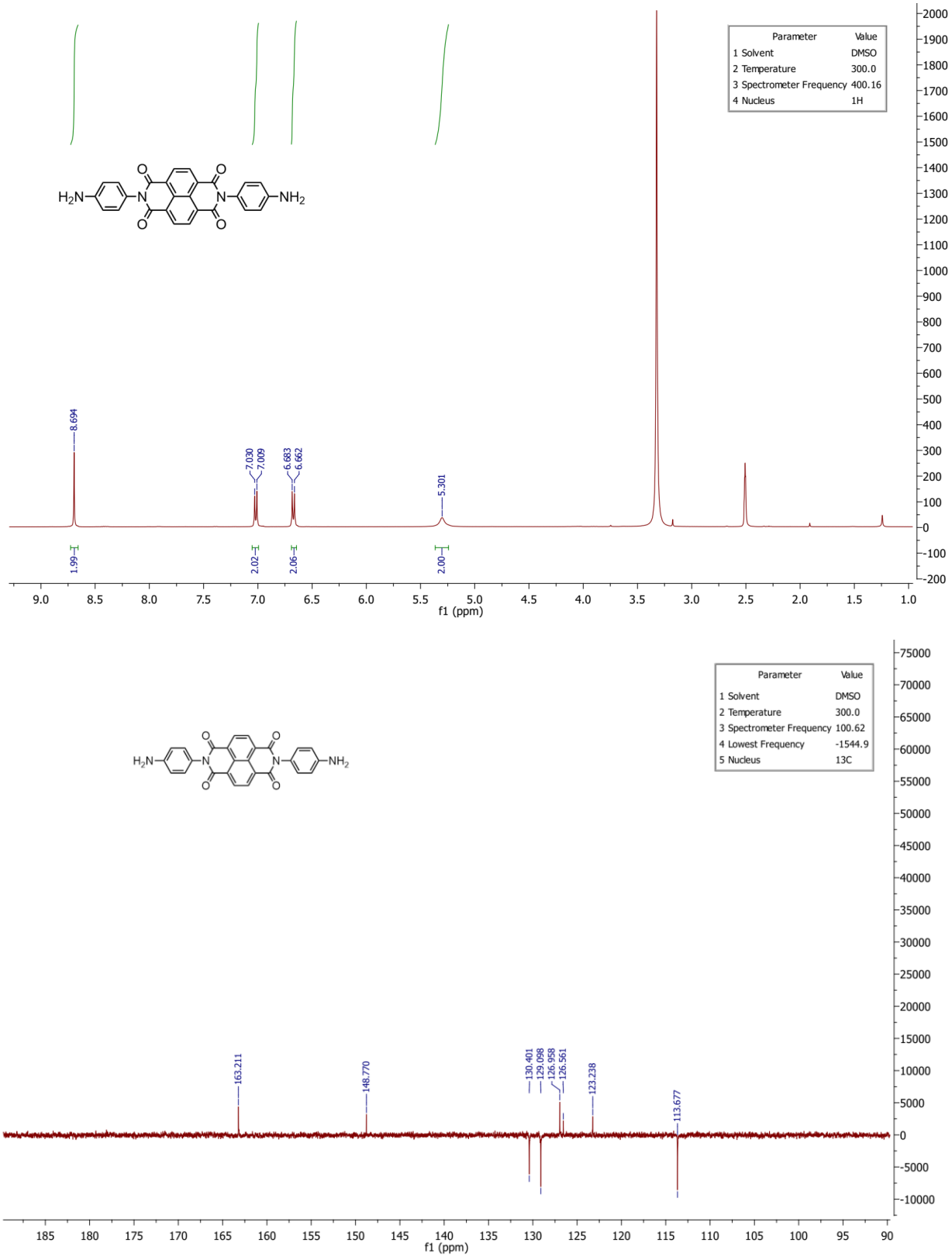

Figure S1. ^{1}H and ^{13}C NMR spectra of NppDI in d^{6}-DMSO.

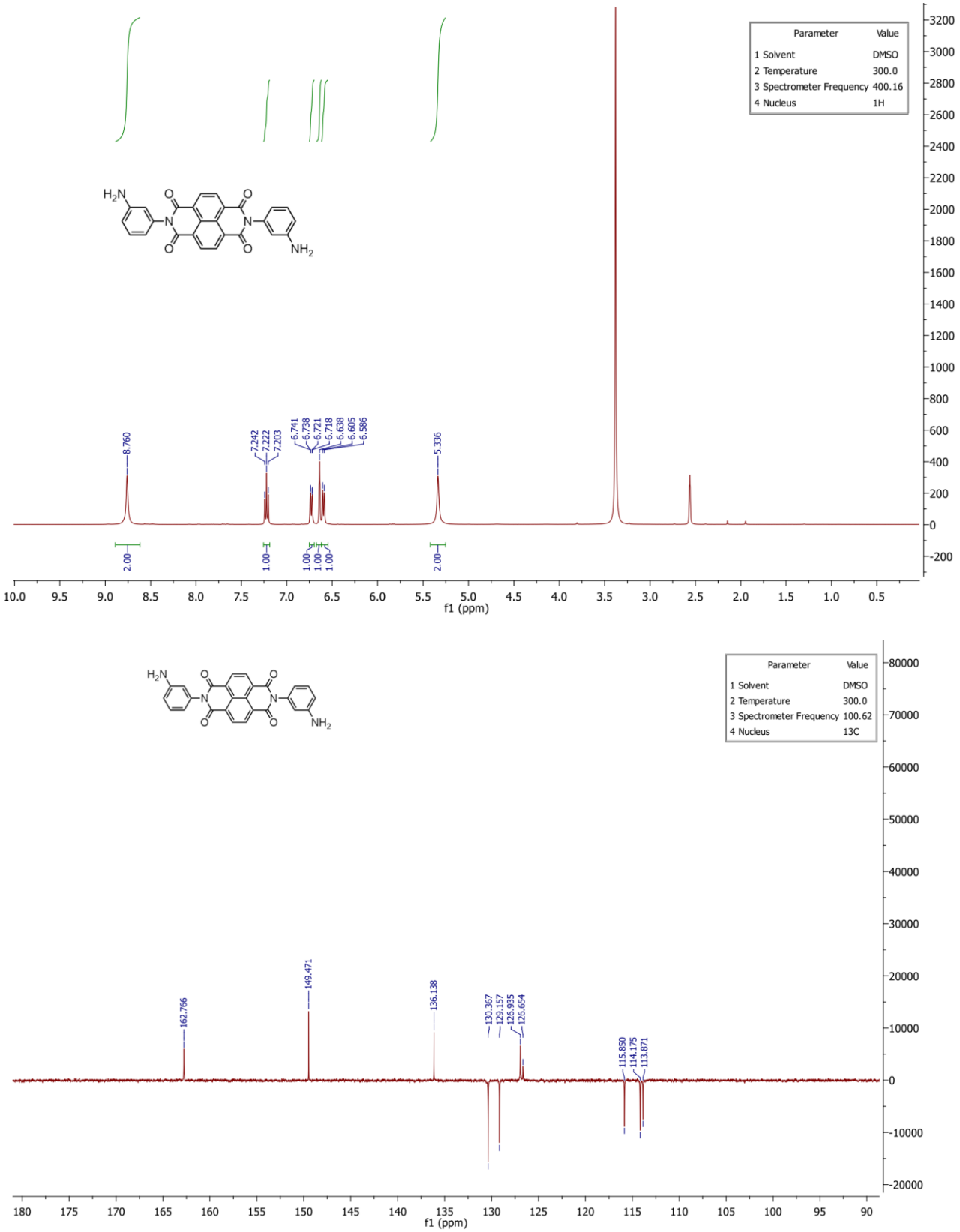

Figure S2. ^{1}H and ^{13}C NMR spectra of NmpDI in d^{6}-DMSO.

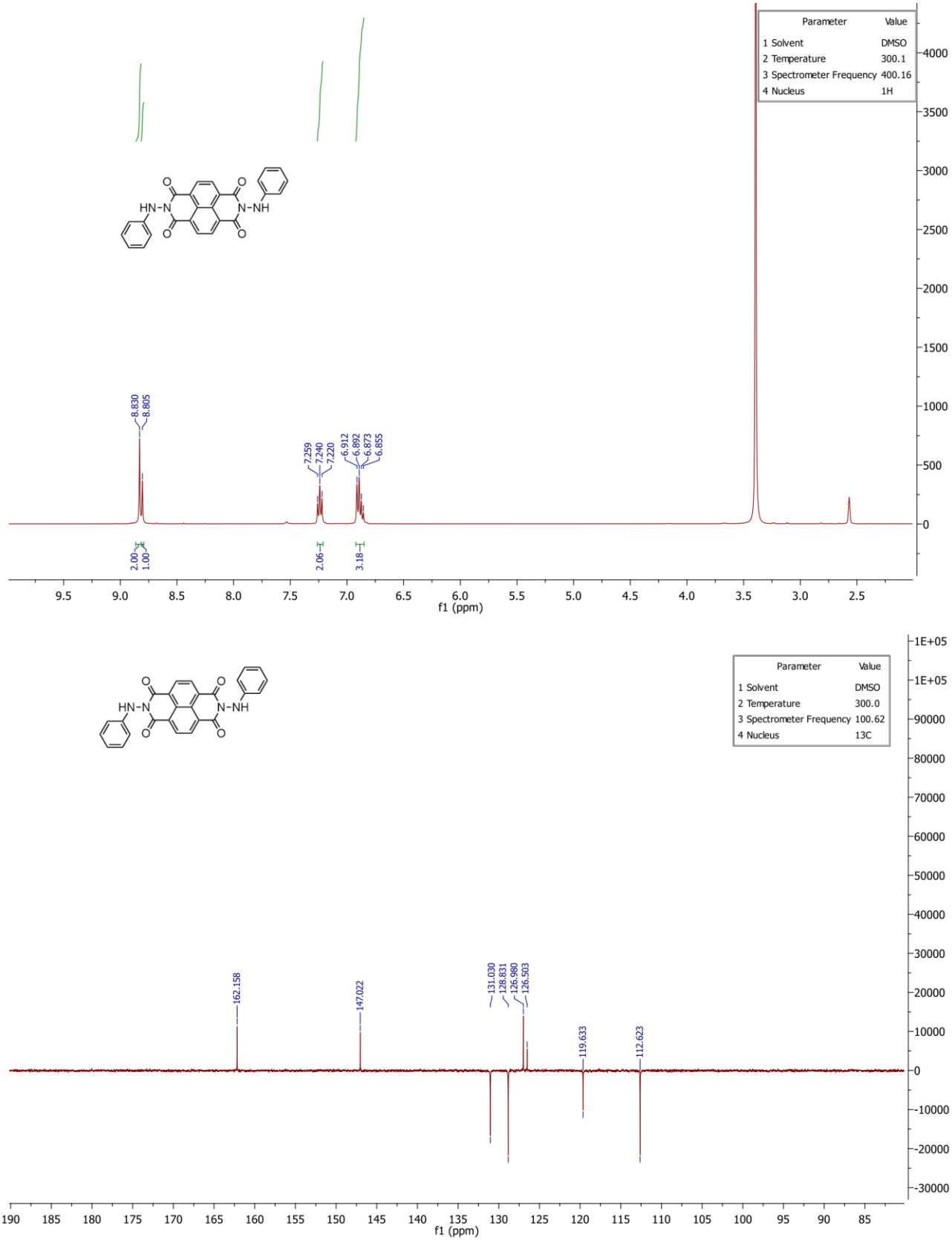

Figure S3. ^{1}H and ^{13}C NMR spectra of NphDI in d^{6}-DMSO

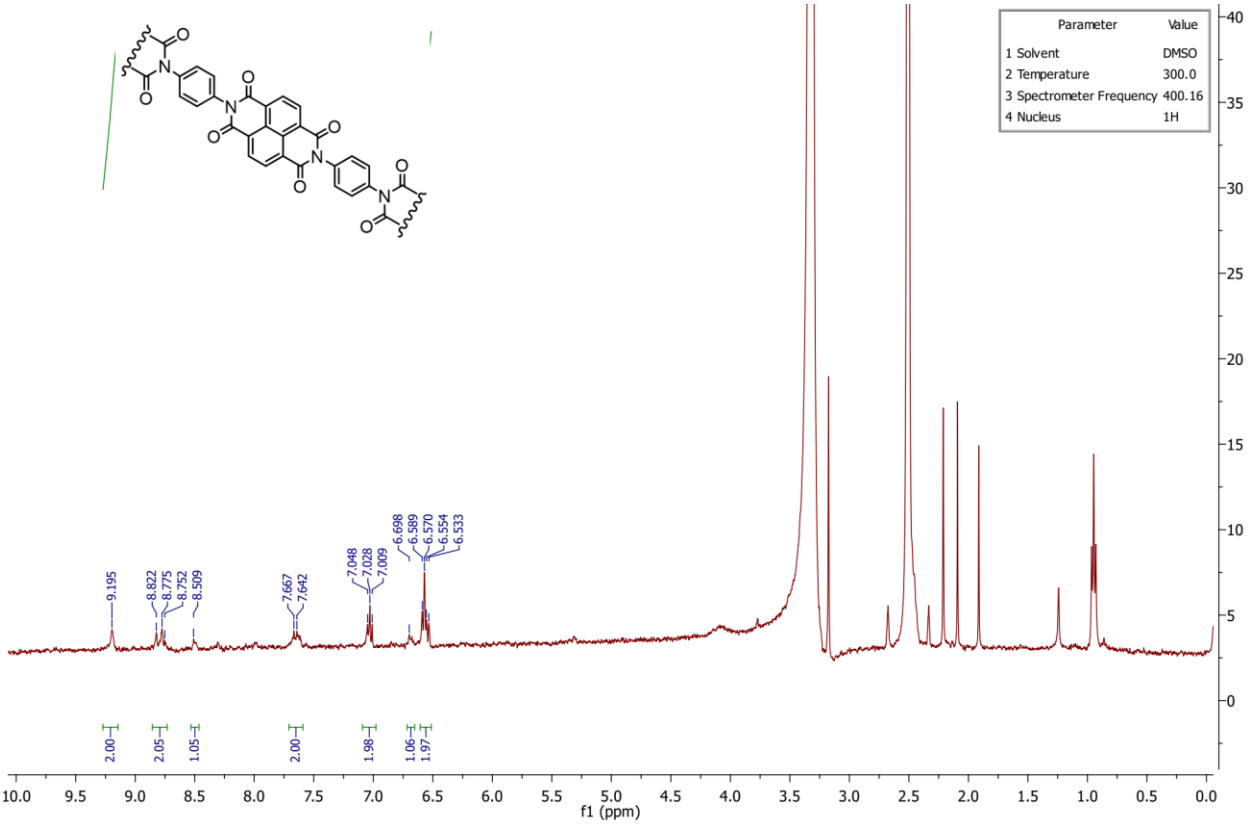

Figure S4. ^{1}H and ^{13}C NMR spectra of the poorly soluble Poly-NppDI in d^{6}-DMSO

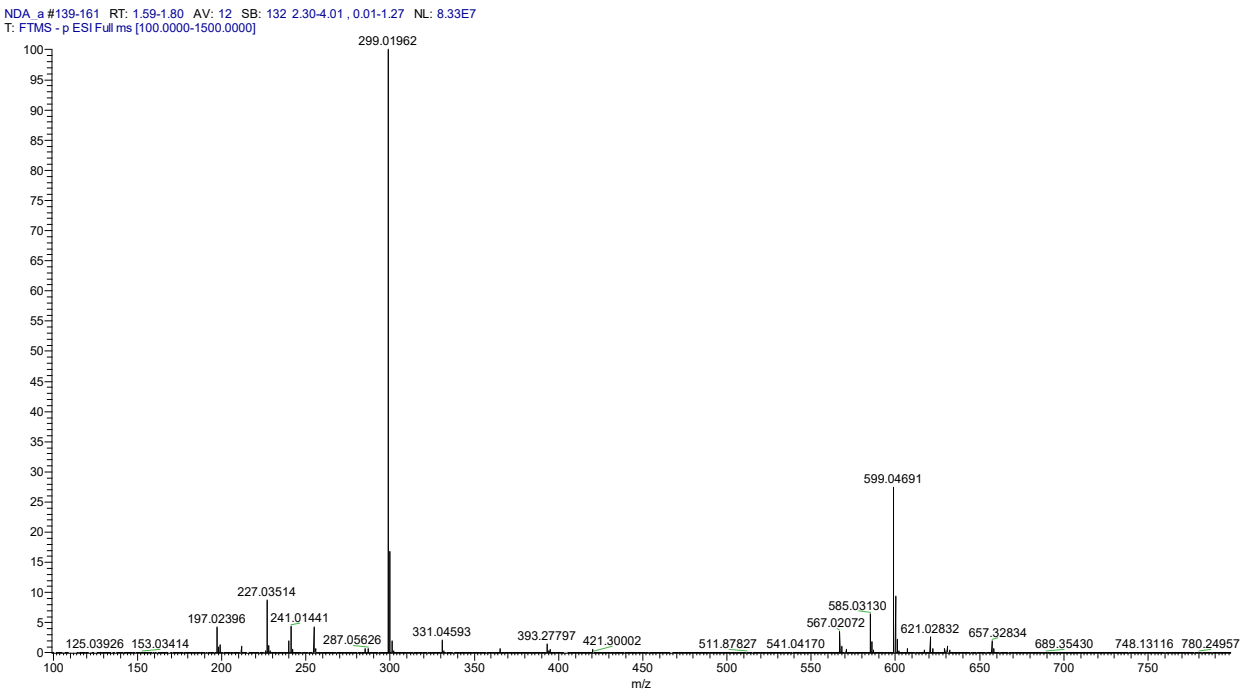

Figure S5. ESI (-) Mass spectrum of NDA: m/z = 299.01 $[M+MeOH]^-$, 599.046 $[2(M+MeOH)]^-$.

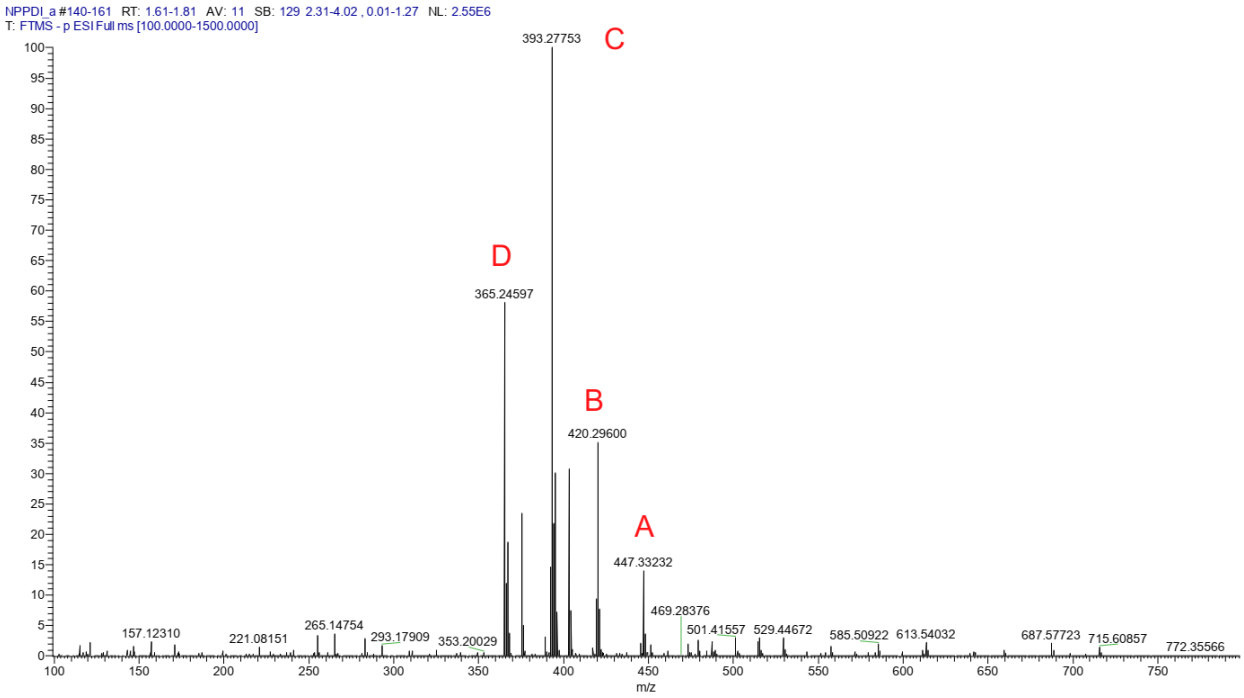

(a)

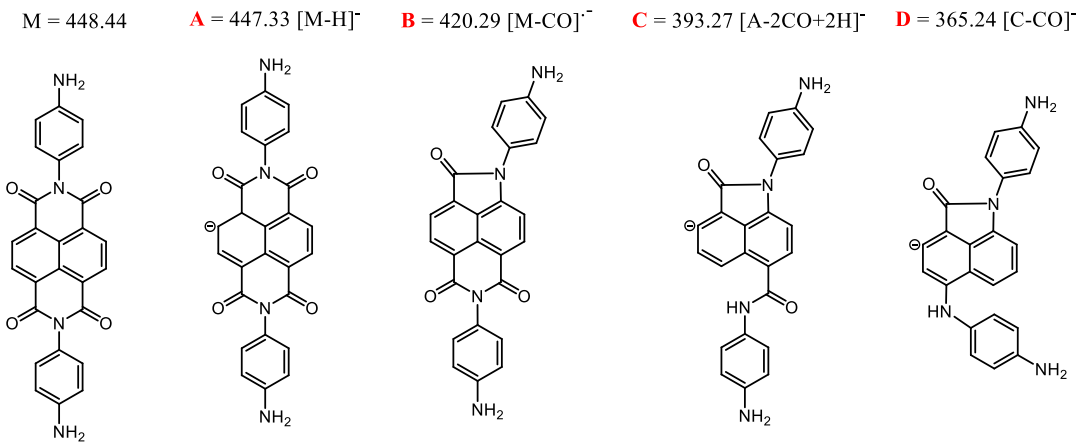

(b)

Figure S6. (a): ESI (-) Mass spectrum of NppDI; (b) interpretation of major peaks, with indication of possible molecular fragmentation and transposition m/z. The same fragmentation scheme is valid for NmpDI and NphDI mass spectra, shown in Figures S7 and S8.

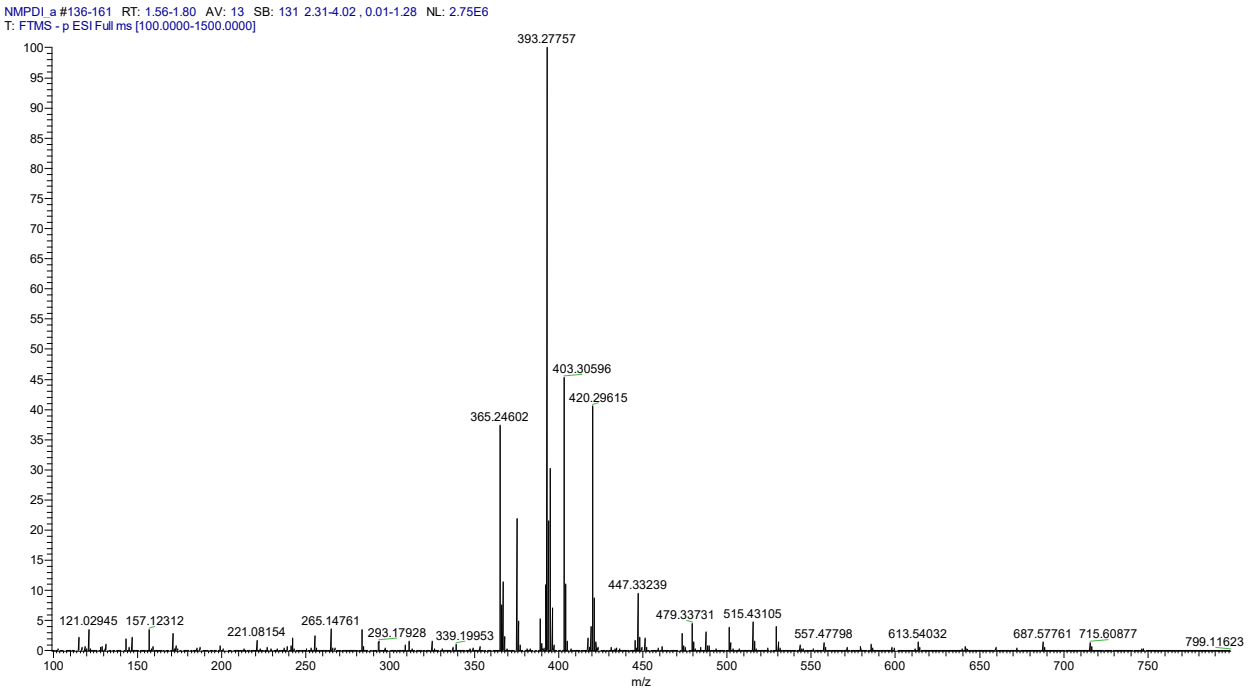

Figure S7. ESI (-) Mass spectrum of NmpDI; peak interpretation as in Figure S6.

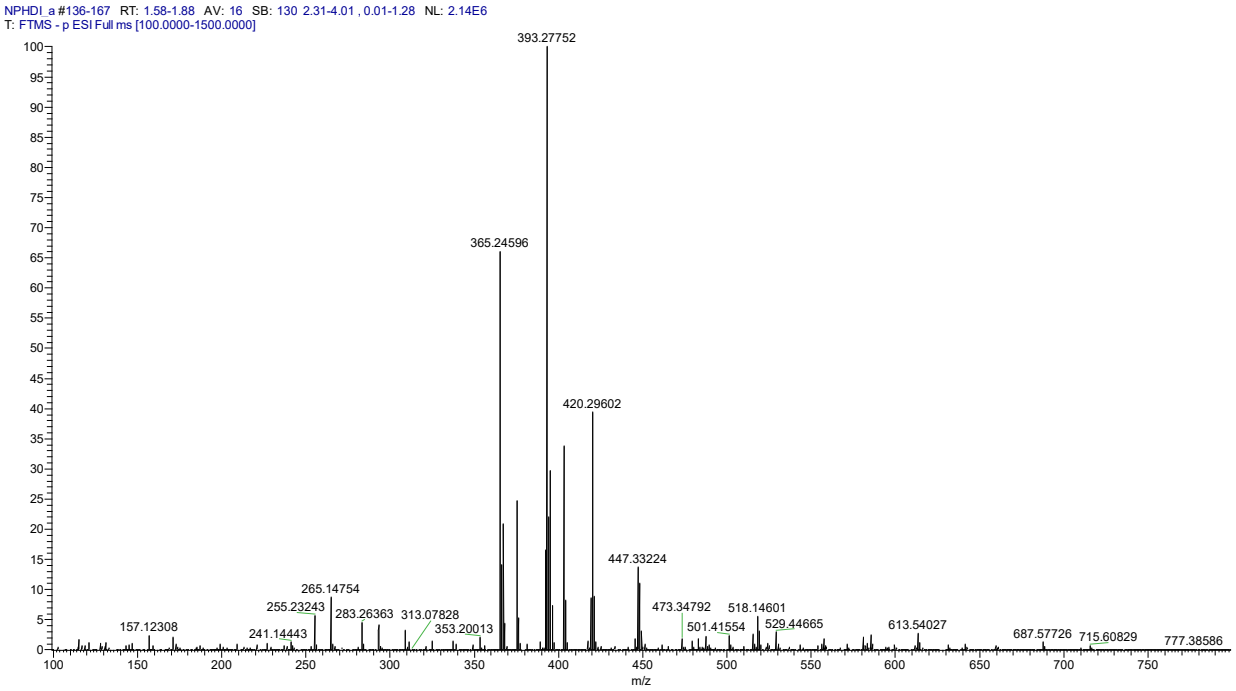

Figure S8. ESI (-) Mass spectrum of NphDI; peak interpretation as in Figure S6.

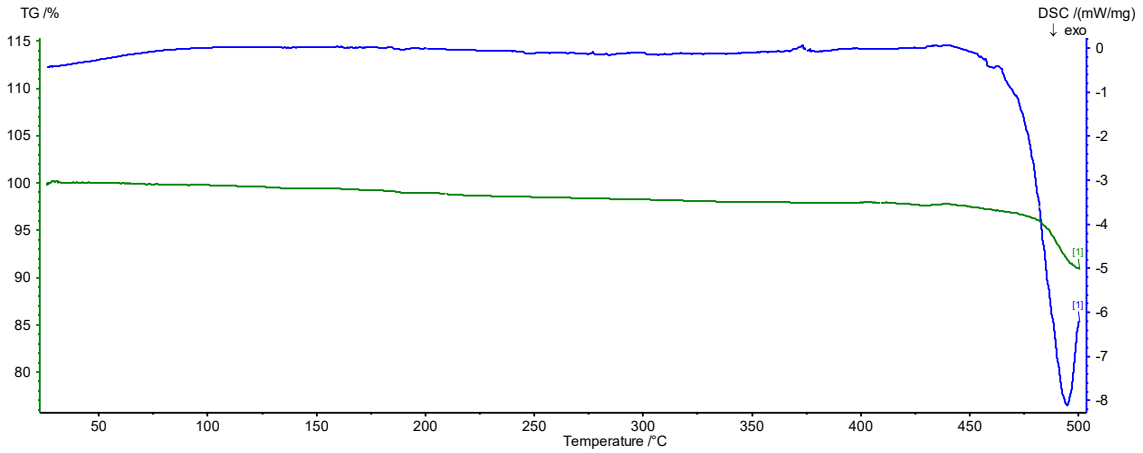
TG /%
DSC /(mW/mg)
↓ exo
115
110
105
100
95
90
85
80
0
-1
-2
-3
-4
-5
-6
-7
-8
50
100
150
200
250
300
350
400
450
500
Temperature /°C

a)

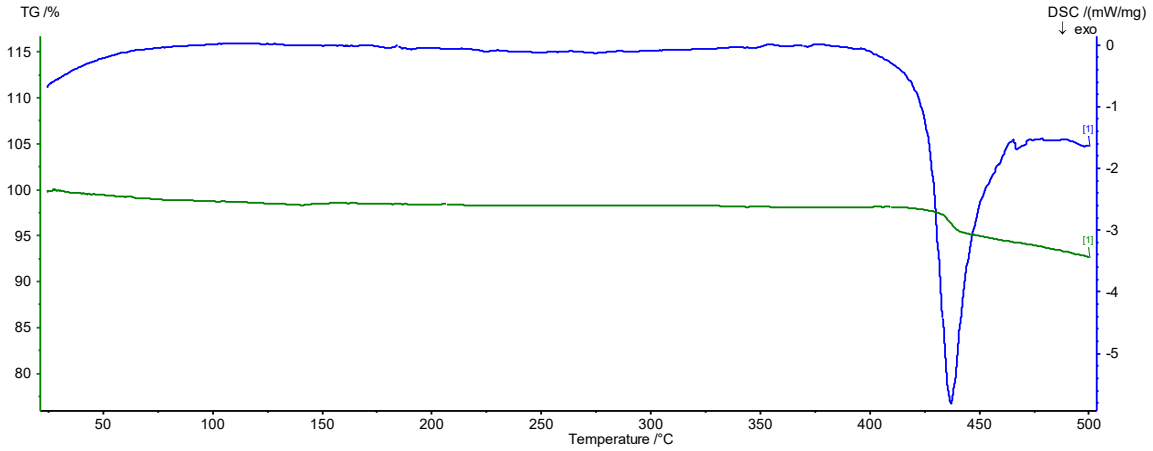
TG /%
DSC /(mW/mg)
↓ exo
115
110
105
100
95
90
85
80
0
-1
-2
-3
-4
-5
50
100
150
200
250
300
350
400
450
500
Temperature /°C

b)

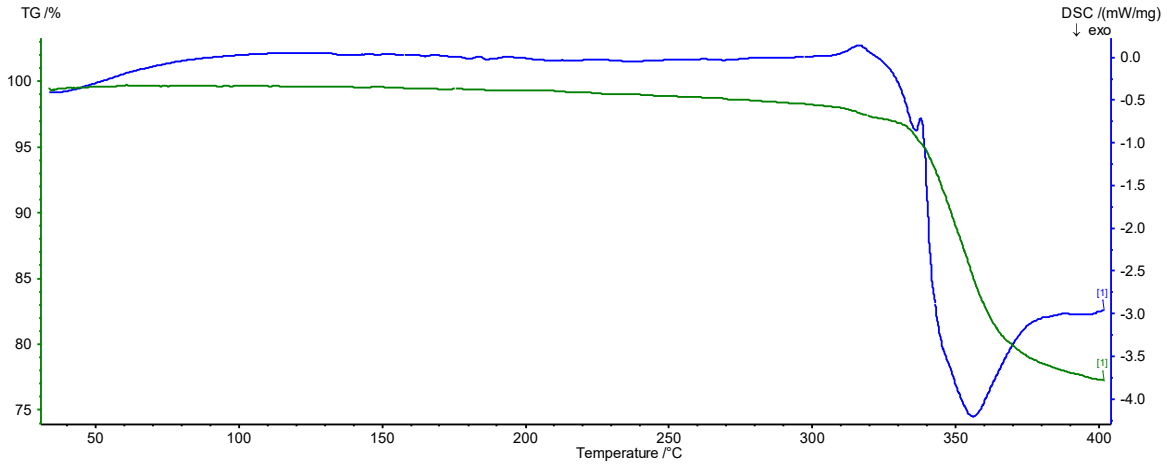
TG /%
DSC /(mW/mg)
↓ exo
100
95
90
85
80
75
0.0
-0.5
-1.0
-1.5
-2.0
-2.5
-3.0
-3.5
-4.0
50
100
150
200
250
300
350
400
Temperature /°C

c)

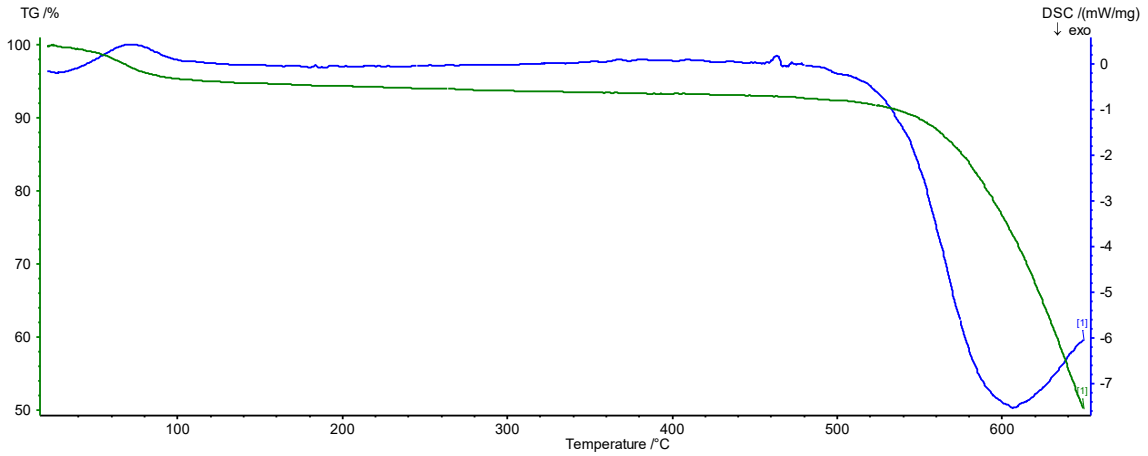

d)

Figure S9. TG traces (in green) and DSC traces (in blue) of the NppDI (a), NmpDI (b), NphDI (c) and Poly-NppDI materials, performed *in air* at a scan rate of 10° min^{-1}. Their extreme stability, with decomposition temperatures above 300°C, and up to 520°C, is evident. In Poly-NppDI (panel d), the small broad endotherm falling below 100°C, accompanied by a 4% weight loss, is attributed to residual solvent molecules.

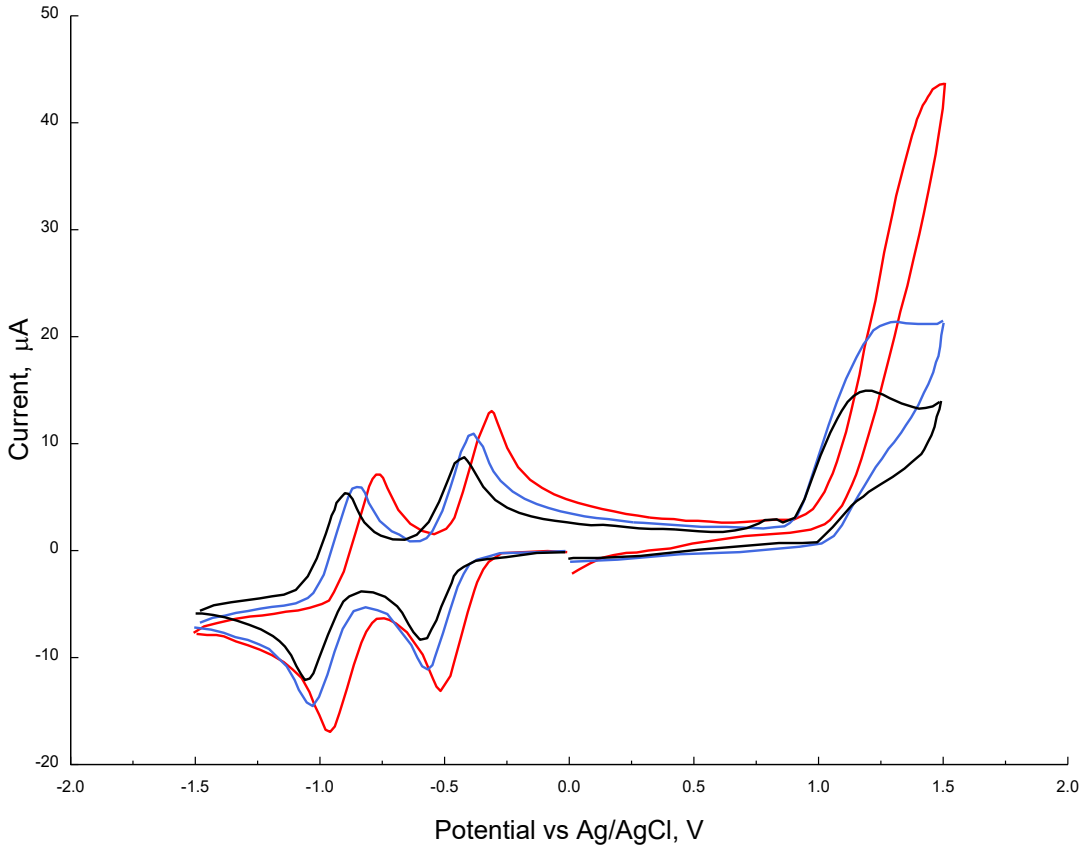

Figure S10. Cyclic voltammograms (in DMSO / 0.1 M $[NBut_4]PF_6$) of the NppDI (black trace), NmpDI (blue trace) and NphDI (red trace) species in ca. 0.15 mg/mL concentrations. Sweeps from -1.5 to 1.5 V, performed at a 0.1 V/s rate.

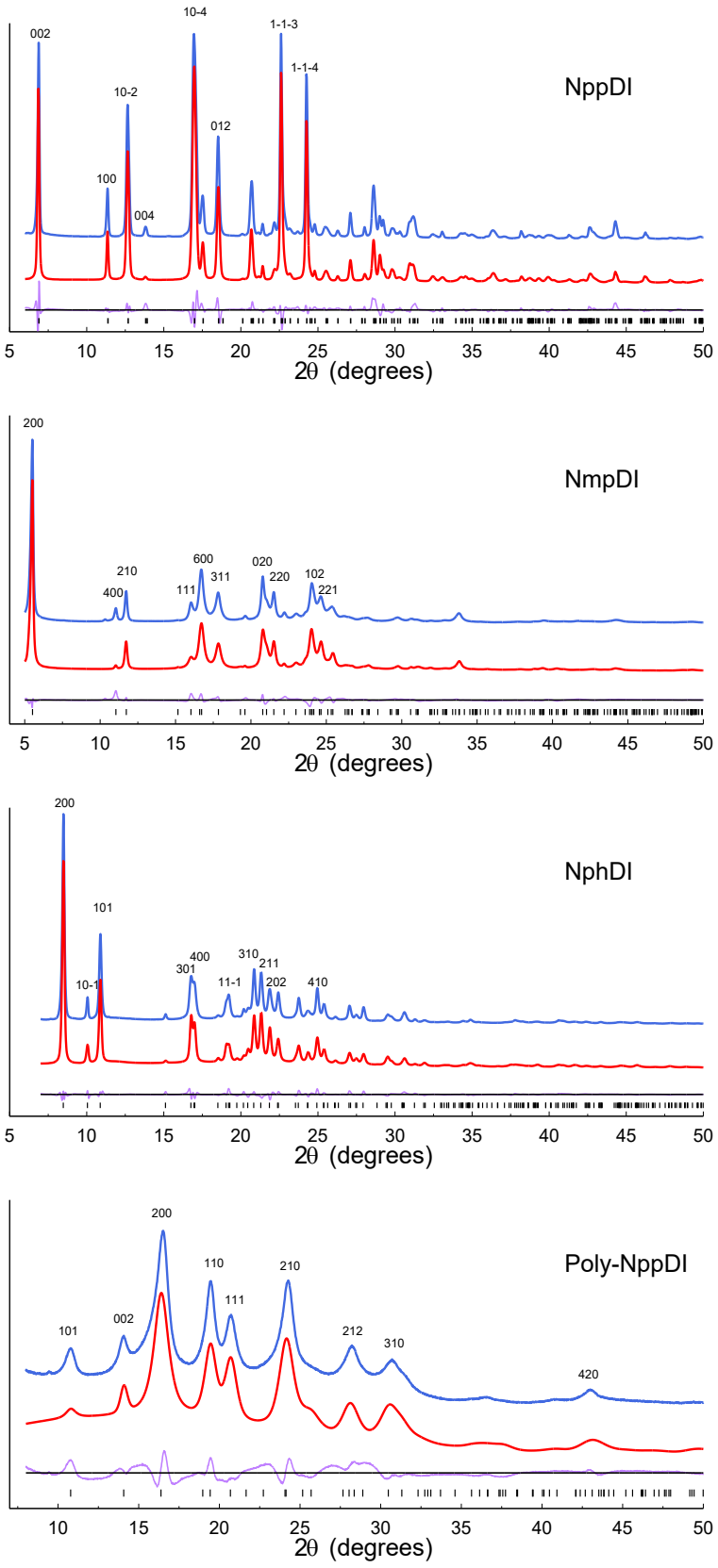

Figure S11: XRPD data (as from Figure 1) with partial labeling of the most characteristic peaks.

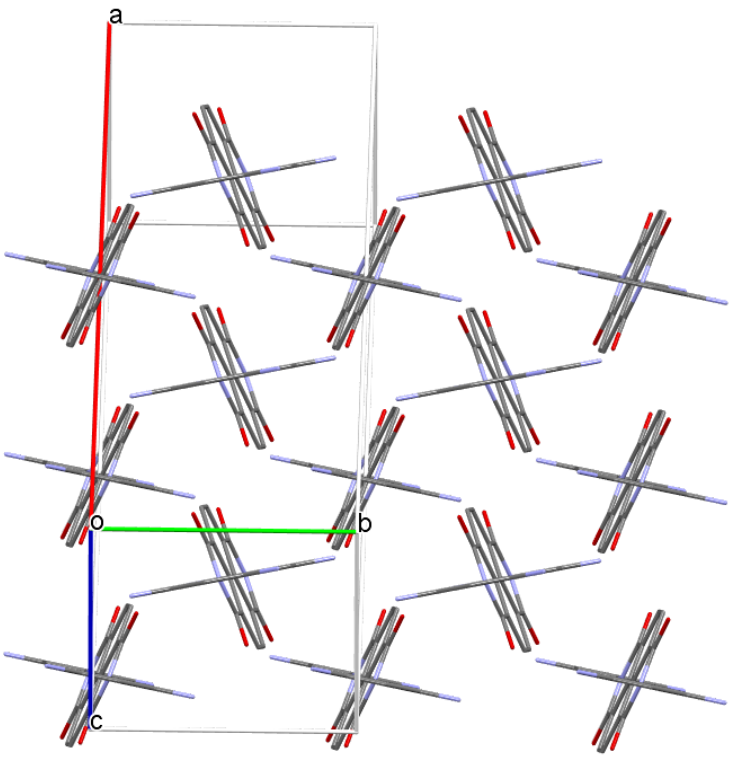

Figure S12: Herringbone motif found in the crystal structure of NmpDI, viewed down [102].

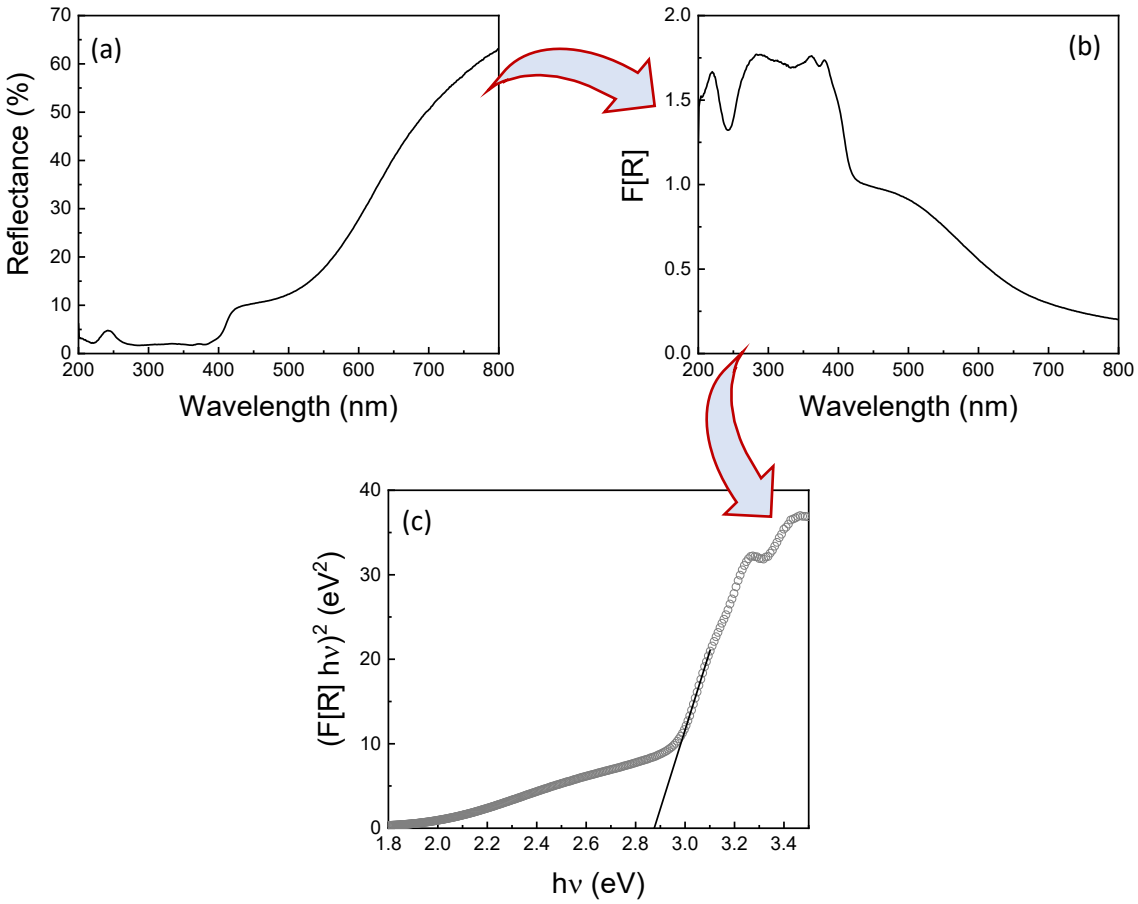

Figure S13: Conversion from the reflectance spectrum (a) of NppDI to Tauc plot (c) passing through the absorbance spectrum (b) in the form of F[R] by the Kubelka-Munk transformation. The Kubelka-Munk function F[R] was calculated from the reflectance spectrum using the $F[R] = (1-R)^2/2R$ relationship. Taking F[R] as representative of the sample absorbance spectrum, the Tauc plot was constructed by representation of $(F[R]\ h\nu)^2$ vs. $h\nu$. The extrapolation of the linear portion of Tauc plot on the $h\nu$ axis provided experimentally accessible direct band gap values.

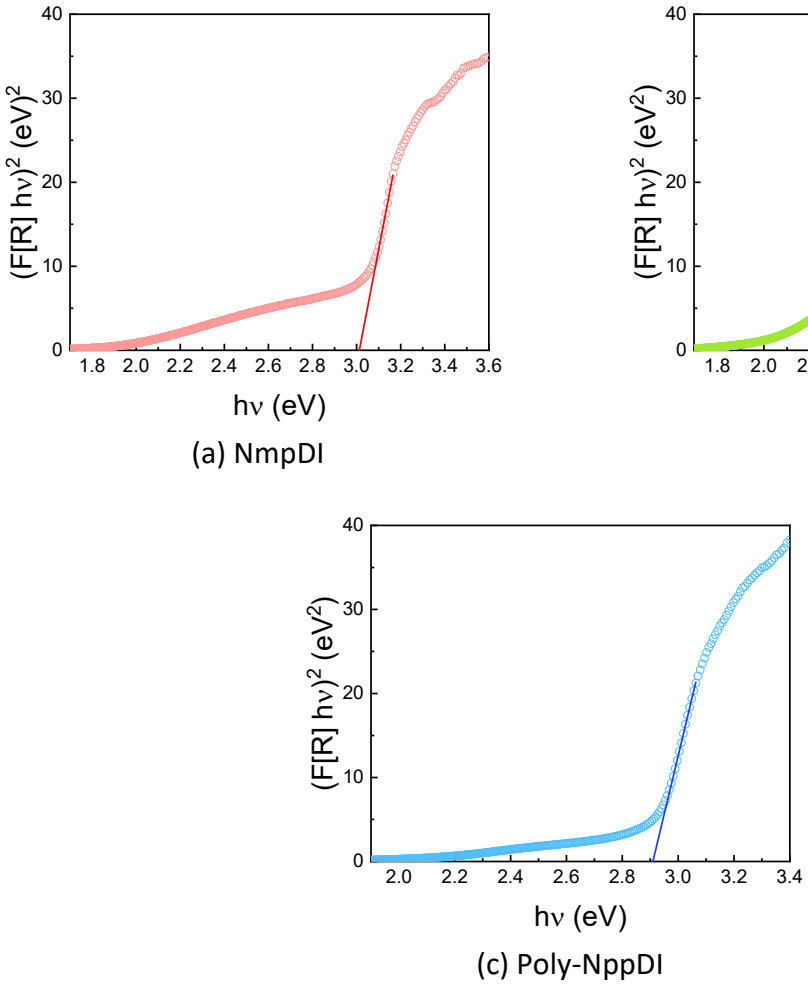

Figure S14: Tauc plots of NmpDI (a), NphDI (b) and Poly-NppDI (c) calculated for a direct band gap transition.

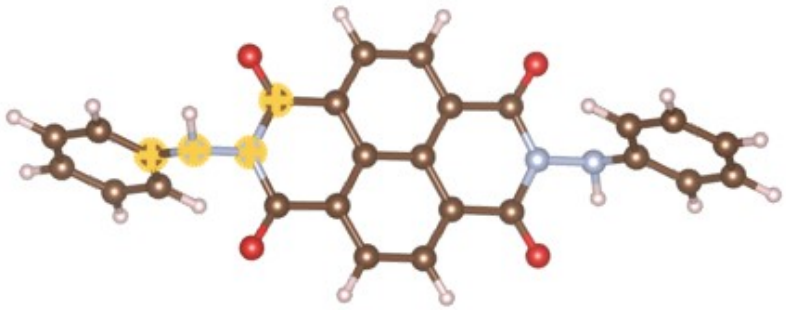

(a)

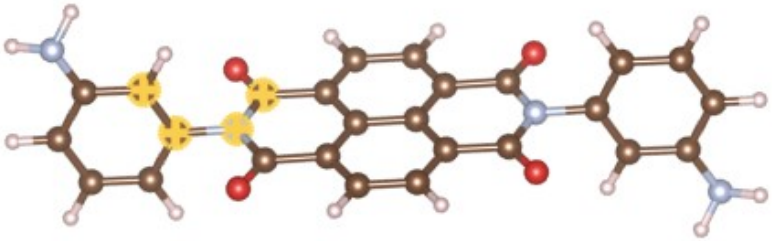

(b)

Figure S15. Optimized structures of NphDI (a) and NmpDI (b) highlighting the four atoms defining the dihedral angle between polyaromatic core plane and side ring plane. H atoms in white, C in brown, N in grey and O in red.

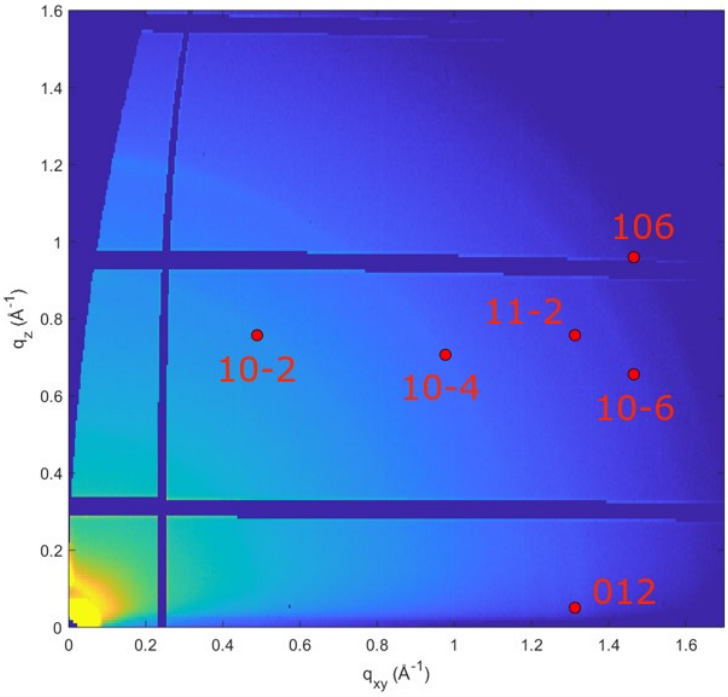

Figure S16:2D-GIXD image of the NppDI thin film taken after thermal annealing and for α_i = 0.05°. In red the theoretical positions of the intensity maxima for film having bulk phase and 001 texturing are highlighted.

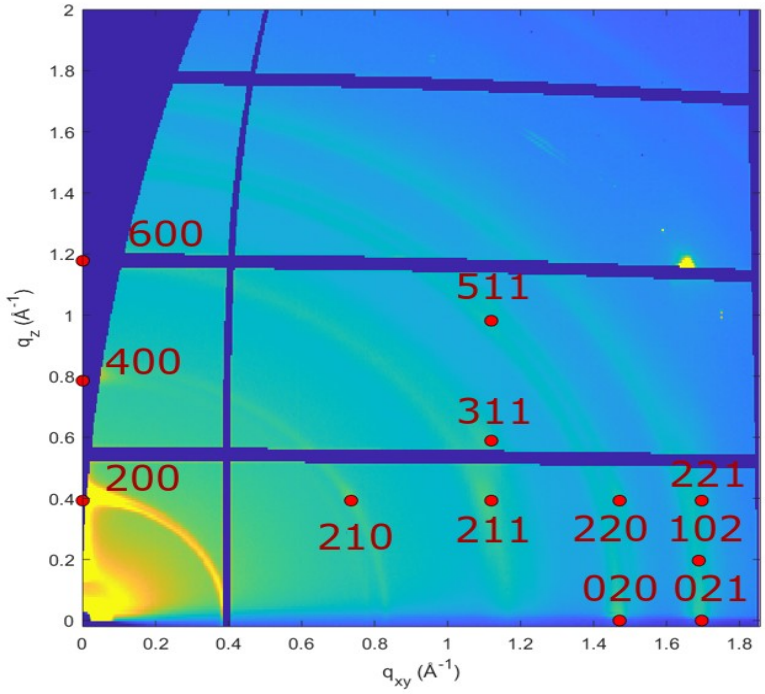

Figure S17: 2D-GIXD image taken for the annealed NmpDI film at α_i = 0.1° with highlighted in red the theoretical positions of the intensity maxima corresponding to (001) texturing of bulk phase.

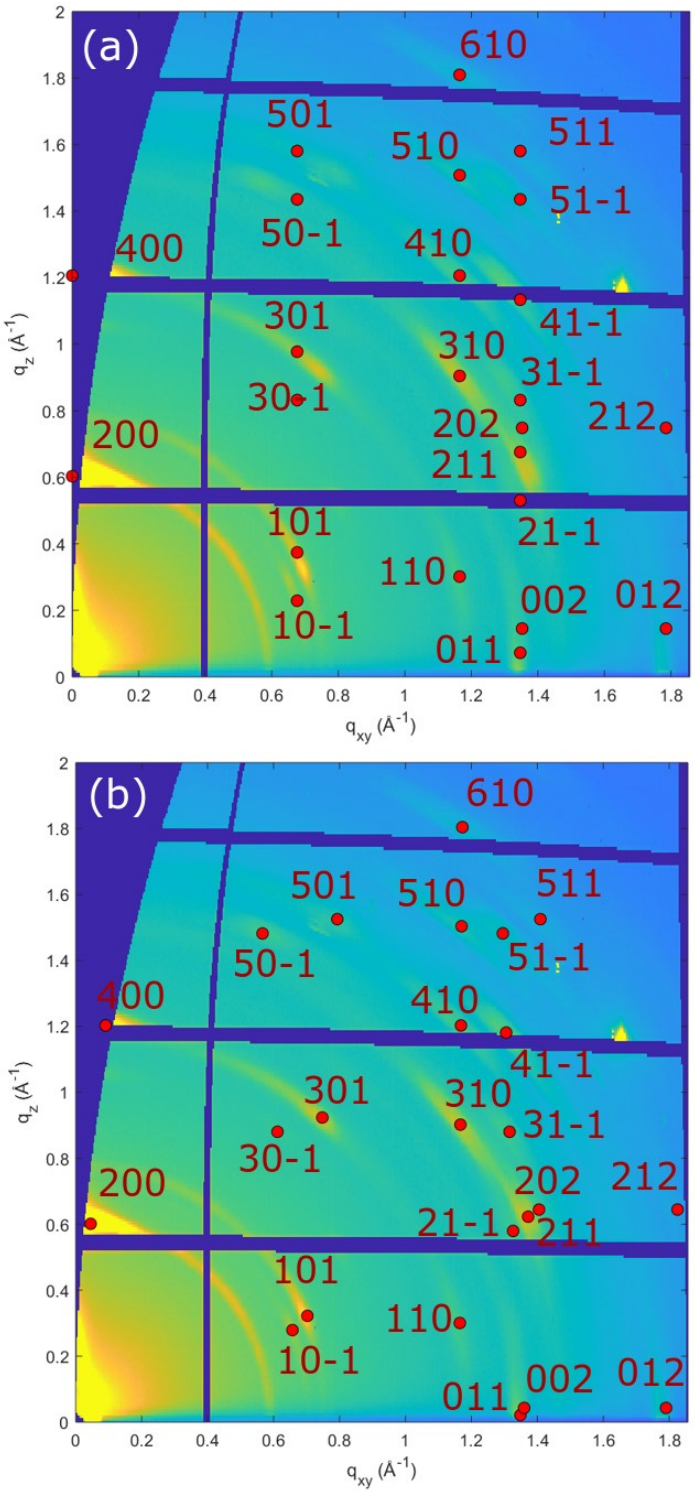

Figure S18: The experimental 2D-GIXD image of the annealed NphDI film at α_i = 0.1° together the theoretical positions of the intensity maxima of the bulk phase (red spots) corresponding to the crystallites having (100) **(a)** parallel or **(b)** tilted by 2.97° with respect to the substrate surface.

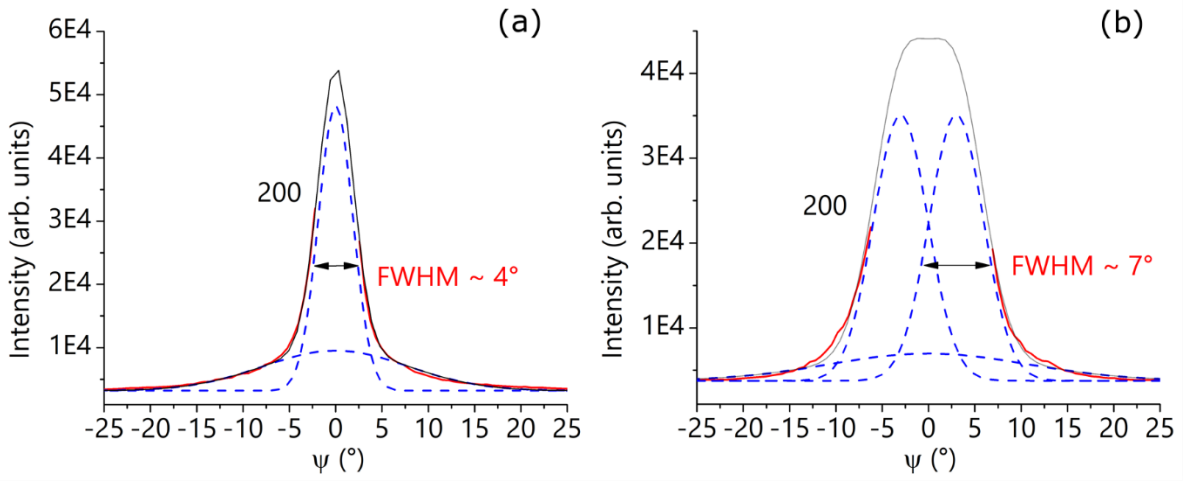

Figure S19: Azimuthal intensity profiles of the 200 reflection for **(a)** NmpDI and **(b)** NphDI films extracted from the corresponding 2D-GIXD images (**Figure S17, S18a**). The solid black lines are the fits to the experimental data (solid red curve) resulting from the convolution of a broad peak (from largely tilted domains) and a narrow one (from highly oriented domains) **(a)**. The last one for NphDI **(b)** splits in two peaks due to the tilt of the (200) with respect to the surface normal.

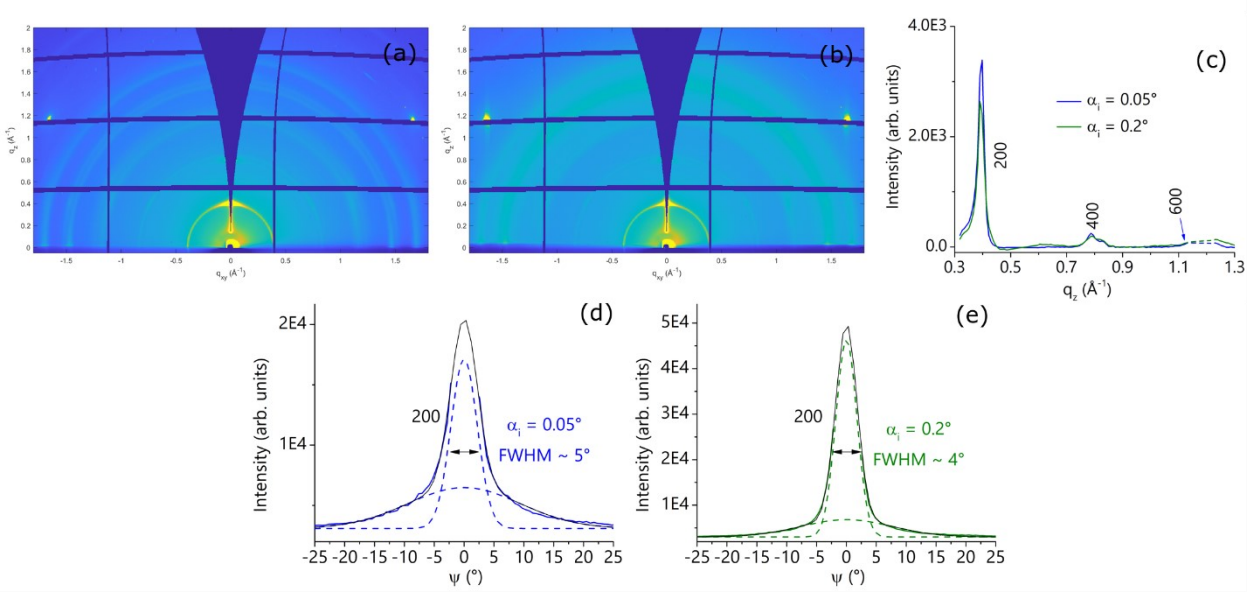

Figure S20: 2D-GIXD images of the annealed NmpDI film recorded at α_i = 0.05° **(a)** and 0.2° (**b**), and the corresponding q_z profiles (**c**). Experimental 200 azimuthal curves (**d** and **e**) extracted respectively from (**a**) and (**b**), together with the fits obtained as explained above (**Figure S19**).

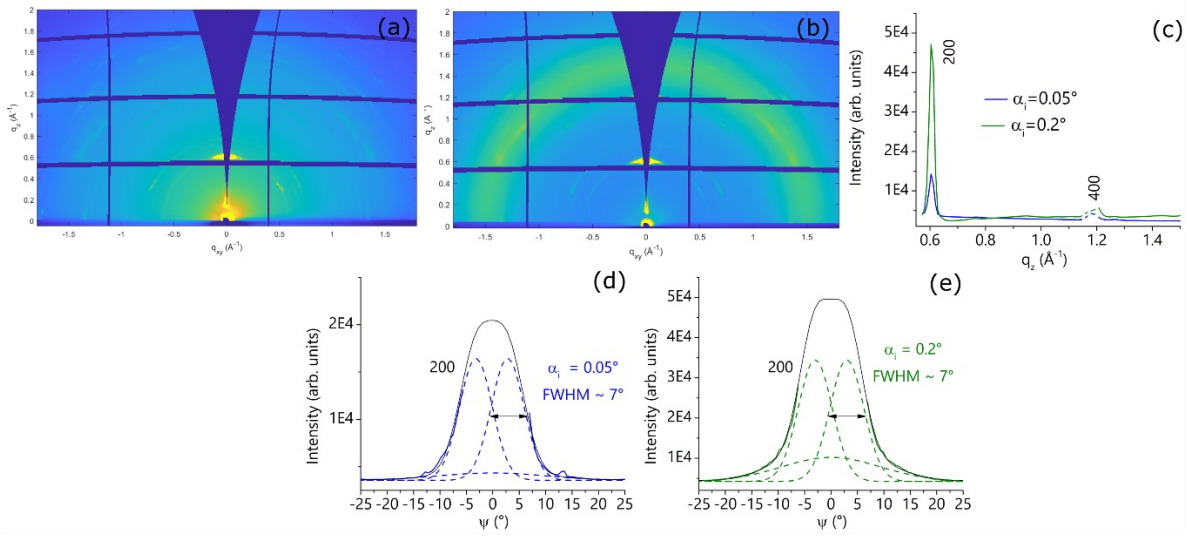

Figure S21: 2D-GIXD images of the annealed NphDI film recorded at α_i = 0.05° (**a**) and 0.2° (**b**), and the corresponding q_z profiles (**c**). For the profile extracted from the 2D image taken at α_i = 0.2° the signal from SiO_2 is subtracted by using a polynomial function Experimental 200 azimuthal curves (**d** and **e**) extracted respectively from (**a**) and (**b**), together with the fits obtained as explained above (**Figure S19**).

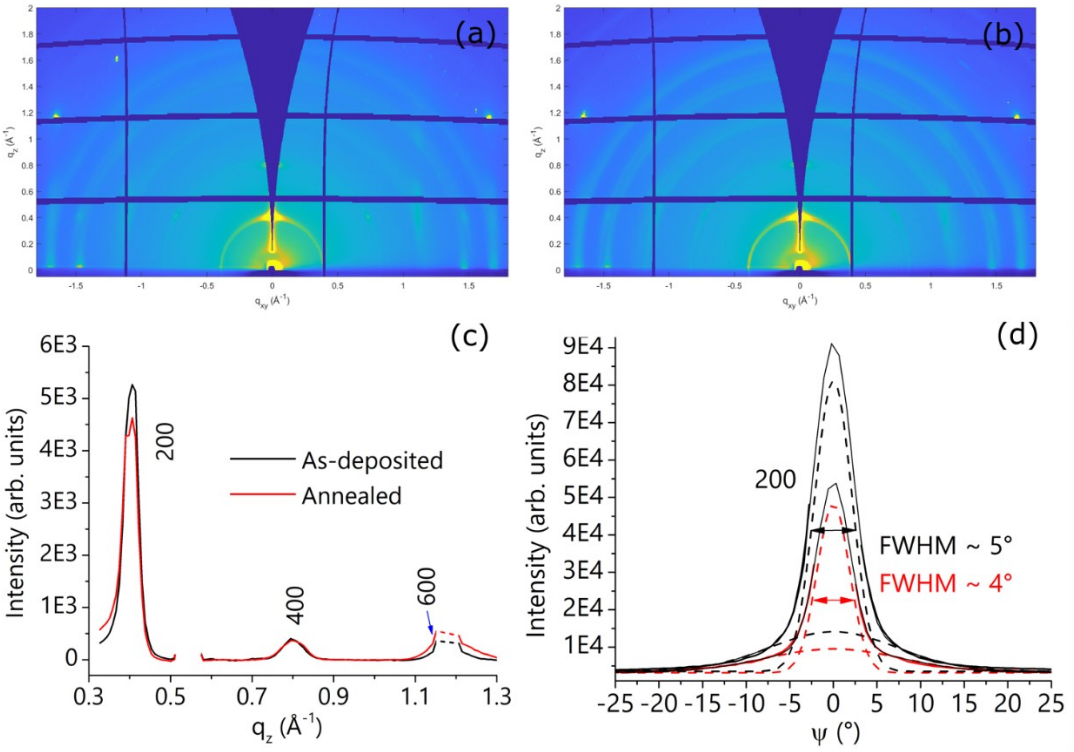

Figure S22: 2D-GIXD images of NmpDI at α_i = 0.1° before (**a**) and after (**b**) the thermal annealing. The corresponding q_z intensity profiles **(c)** and the 200 azimuthal profiles (**d**) before (black) and after (red) the annealing. The fits in (**d**) are obtained as explained above (**Figure S19**).

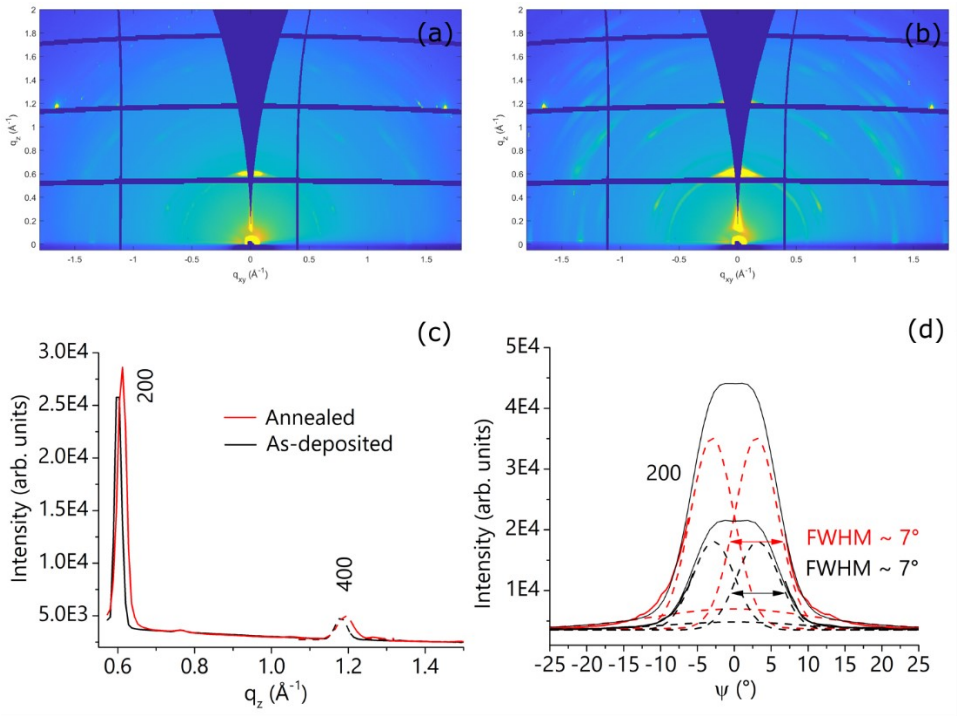

Figure S23: 2D-GIXD images taken with $\alpha_i = 0.1°$ for the NphDI film before (a) and after (b) thermal annealing. The extracted q_z intensity profiles **(c)** show a slight shift of the (200) of the as-deposited curve towards lower q_z, likely due to solvent presence able to induce a lattice expansion of ~ 0.8% as compared to the theoretical unit cell. After annealing, the position of the 200 peak matches the theoretical value for the undeformed unit cell. (d) Experimental 200 azimuthal profiles before (black) and after (red) thermal annealing, together with the fits obtained as explained above (**Figure S19**).

Table S1. Solubility tests. Italics indicate solubilities < 1 mg/mL.

Species	Soluble in	Insoluble in
NphDI	*DMSO, NMP, DMSO/DMF 1:1, DMF/NMP 1.1, NMP/Acetone*	DMF, CH_3CN, Toluene, Et_2O, THF, MeOH, Dioxane, CH_2Cl_2, $CHCl_3$, CCl_4, AcOEt
NppDI	DMSO, DMF, DMA	CH_3CN, Toluene, Et_2O, THF, MeOH, Dioxane, CH_2Cl_2, $CHCl_3$, CCl_4, AcOEt
NmpDI	DMF, THF, *CH_3CN*, $CHCl_3$	Toluene, Et_2O, THF, MeOH, Dioxane, CH_2Cl_2, CCl_4, AcOEt

Table S2. Optimized structure of the isolated NphDI molecule [cartesian xyz coordinates, Å].			
C	-0.68366	0.01967	0.19372
C	-1.36609	1.26127	0.20101
C	-0.70771	2.42361	-0.16666
H	-1.25503	3.35956	-0.14897
C	-1.33537	-1.18194	0.56838
C	-0.6444	-2.38287	0.55415
H	-1.16959	-3.28565	0.8457
C	-2.79089	1.3208	0.6101
C	-2.76733	-1.17165	0.97874
O	-3.4182	2.36278	0.71405
O	-3.36853	-2.17314	1.3106
N	-3.40566	0.08932	0.91612
C	-5.75122	0.02271	0.36755
C	-6.99662	0.6072	0.63542
C	-8.04718	0.45973	-0.26562
C	-7.87257	-0.2664	-1.44563
C	-6.63249	-0.84761	-1.70735
C	-5.57378	-0.71253	-0.80872
N	-4.73554	0.14507	1.35583
H	-7.13804	1.17672	1.55052
H	-9.00485	0.92233	-0.04555
H	-6.48113	-1.41882	-2.61871
H	-4.62223	-1.18427	-1.0222
H	-8.69169	-0.37748	-2.14885
H	-4.84232	1.00374	1.8873
C	0.6837	-0.01964	-0.19382

C	1.36612	-1.26124	-0.2011
C	0.70775	-2.42358	0.16658
H	1.25506	-3.35953	0.14889
C	1.33541	1.18197	-0.56847
C	0.64444	2.3829	-0.55422
H	1.16963	3.28568	-0.84577
C	2.79091	-1.32078	-0.61021
C	2.76737	1.17168	-0.97881
O	3.41824	-2.36275	-0.71408
O	3.36859	2.17319	-1.3106
N	3.40569	-0.08929	-0.9162
C	5.75121	-0.02272	-0.36751
C	6.99662	-0.60721	-0.63532
C	8.04712	-0.45978	0.2658
C	7.87244	0.2663	1.44582
C	6.63235	0.8475	1.70748
C	5.5737	0.71247	0.80878
N	4.73559	-0.14503	-1.35585
H	7.1381	-1.17669	-1.55044
H	9.00481	-0.92238	0.04577
H	6.48093	1.41868	2.61886
H	4.62213	1.1842	1.02221
H	8.69151	0.37734	2.1491
H	4.84241	-1.00365	-1.88739

Table S3. Optimized structure of the isolated NppDI molecule [cartesian xyz coordinates, Å].			
C	0.71101	-0.00166	-0.00011
C	1.40383	-1.23523	-0.04859
C	0.69806	-2.4268	-0.09624
H	1.25499	-3.3565	-0.13353
C	1.40962	1.22869	0.04821
C	0.70932	2.4235	0.09608
H	1.27046	3.35067	0.13327
C	2.89236	-1.25978	-0.04961
C	2.89819	1.24619	0.04889
O	3.526	-2.29999	-0.08939
O	3.53669	2.28373	0.0892
N	3.54376	-0.00811	-0.00086
C	4.99065	-0.01091	-0.00139
C	5.69012	0.17739	-1.19209
C	7.07989	0.18353	-1.1947
C	7.79893	-0.00228	-0.00069
C	7.08048	-0.19468	1.19256
C	5.69061	-0.19716	1.18924
N	9.19092	-0.05113	-0.00885
H	5.14452	0.32471	-2.11865
H	7.61753	0.32958	-2.12768
H	7.61848	-0.34574	2.12457
H	5.14553	-0.3431	2.11633
H	9.6376	0.4217	-0.78199
H	9.63777	0.15653	0.87323
C	-0.71101	0.00166	0.0001

C	-1.40383	1.23523	0.04859
C	-0.69806	2.4268	0.09624
H	-1.25499	3.3565	0.13353
C	-1.40962	-1.22869	-0.04822
C	-0.70932	-2.4235	-0.09608
H	-1.27046	-3.35067	-0.13328
C	-2.89236	1.25978	0.0496
C	-2.89819	-1.24618	-0.0489
O	-3.526	2.29999	0.08938
O	-3.53669	-2.28373	-0.0892
N	-3.54376	0.00811	0.00086
C	-4.99065	0.01091	0.00139
C	-5.69012	-0.17738	1.19209
C	-7.07989	-0.18353	1.19471
C	-7.79893	0.00228	0.00069
C	-7.08048	0.19468	-1.19256
C	-5.69061	0.19715	-1.18924
N	-9.19092	0.05113	0.00886
H	-5.14452	-0.3247	2.11865
H	-7.61752	-0.32957	2.12769
H	-7.61848	0.34573	-2.12457
H	-5.14553	0.34309	-2.11633
H	-9.6376	-0.4217	0.782
H	-9.63777	-0.15654	-0.87322

Table S4. Optimized structure of the isolated NmpDI molecule [cartesian xyz coordinates, Å].			
C	-0.70966	-0.01449	-0.0411
C	-1.41998	1.19472	-0.23506
C	-0.73396	2.39374	-0.34475
H	-1.30377	3.30421	-0.49394
C	-1.38765	-1.25207	0.07269
C	-0.67076	-2.42244	0.26349
H	-1.21677	-3.35553	0.34802
C	-2.90582	1.18563	-0.32295
C	-2.87296	-1.30367	-0.01167
O	-3.55569	2.20397	-0.48547
O	-3.49579	-2.34668	0.08156
N	-3.53422	-0.07216	-0.20684
C	-4.98117	-0.10374	-0.30318
C	-5.73615	0.21907	0.81854
C	-7.13829	0.20789	0.74813
C	-7.74744	-0.14444	-0.46869
C	-6.97327	-0.46876	-1.57858
C	-5.58032	-0.44949	-1.5121
N	-7.90642	0.48441	1.87879
H	-5.23665	0.4832	1.74571
H	-8.83203	-0.16438	-0.53648
H	-7.46337	-0.73667	-2.50971
H	-4.97059	-0.69808	-2.37309
H	-7.4535	1.05631	2.5782
H	-8.84902	0.79671	1.69098
C	0.70966	0.01449	0.04109

C	1.41998	-1.19472	0.23506
C	0.73396	-2.39374	0.34475
H	1.30377	-3.30421	0.49394
C	1.38765	1.25208	-0.0727
C	0.67076	2.42244	-0.2635
H	1.21677	3.35553	-0.34803
C	2.90582	-1.18562	0.32296
C	2.87296	1.30367	0.01164
O	3.55569	-2.20397	0.48547
O	3.49579	2.34668	-0.08156
N	3.53422	0.07216	0.20684
C	4.98117	0.10374	0.30318
C	5.73616	-0.21909	-0.81854
C	7.13829	-0.2079	-0.74812
C	7.74744	0.14444	0.46869
C	6.97326	0.46878	1.57858
C	5.58032	0.44952	1.5121
N	7.90643	-0.48445	-1.87877
H	5.23665	-0.48324	-1.7457
H	8.83203	0.16438	0.53649
H	7.46337	0.73671	2.5097
H	4.97058	0.69812	2.37308
H	7.4535	-1.05636	-2.57817
H	8.84903	-0.79675	-1.69095

Table S5. Dihedral angles between the core polyaromatic ring plane and the side ring plane, in the experimental crystal structure (Crystal) and in the optimized isolated molecules (Opt.).

Species	Dihedral angle (°)	
	Crystal	**Opt.**
NphDI	95.18	92.29
NppDI	97.34	96.81
NmpDI	78.41	81.12

Table S6. Electrochemical properties of molecular species. E values vs. Ag/AgCl electrode.

Species	$E_{onset\ red}$, V	E^0_{red1}, V	E^0_{red2}, V	$E_{onset\ ox}$, V	EA, eV	IP, eV	ΔEg_{el}, V
NphDI	-0.39	-0.41	-0.86	1.02	4.01	5.42	1.41
NppDI	-0.43	-0.48	-0.97	0.90	3.97	5.30	1.33
NmpDI	-0.44	-0.51	-0.97	0.90	3.96	5.30	1.34

$E_{onset\ red}$ = onset reduction potential.
$E_{onset\ ox}$ = onset oxidation potential.
EA = electron affinity: EA = $|e^-|(4.4+ E_{onset\ ox})$.
IP = ionization potential: IP = $|e^-|(4.4+ E_{onset\ red})$.
ΔEg_{el} = electrochemical band gap: ΔEg_{el} = IP-EA.
Note: the Ag/AgCl electrode has been set -4.4 eV away from the zero vacuum-level.